*Published online 8 March 2012* *Nucleic Acids Research, 2012, Vol. 40, No. 12* ***5497–5510***
*doi:10.1093/nar/gks222*

# CBX4-mediated SUMO modification regulates BMI1 recruitment at sites of DNA damage

**Ismail Hassan Ismail[1,2], Jean-Philippe Gagné[3], Marie-Christine Caron[4], Darin McDonald[1], Zhizhong Xu[1], Jean-Yves Masson[4], Guy G. Poirier[3] and Michael J. Hendzel[1,*]**

[1]Department of Oncology, Faculty of Medicine and Dentistry, University of Alberta, 11560 University Avenue, Edmonton, Alberta, Canada, [2]Biophysics Department, Faculty of Science, Cairo University, 12613 Giza, Egypt, [3]Proteomics Platform of the Quebec Genomics Center, Centre de recherche du CHUQ—CRCHUL, 2705 Boulevard Laurier, Québec, Canada, G1V 4G2 and [4]Genome Stability Laboratory, Laval University Cancer Research Center, Hôtel-Dieu de Québec, Quebec City, Quebec, Canada

Received October 10, 2011; Revised February 16, 2012; Accepted February 21, 2012

## ABSTRACT

**Polycomb group (PcG) proteins are involved in epigenetic silencing where they function as major determinants of cell identity, stem cell pluripotency and the epigenetic gene silencing involved in cancer development. Recently numerous PcG proteins, including CBX4, have been shown to accumulate at sites of DNA damage. However, it remains unclear whether or not CBX4 or its E3 sumo ligase activity is directly involved in the DNA damage response (DDR). Here we define a novel role for CBX4 as an early DDR protein that mediates SUMO conjugation at sites of DNA lesions. DNA damage stimulates sumoylation of BMI1 by CBX4 at lysine 88, which is required for the accumulation of BMI1 at DNA damage sites. Moreover, we establish that CBX4 recruitment to the sites of laser micro-irradiation-induced DNA damage requires PARP activity but does not require H2AX, RNF8, BMI1 nor PI-3-related kinases. The importance of CBX4 in the DDR was confirmed by the depletion of CBX4, which resulted in decreased cellular resistance to ionizing radiation. Our results reveal a direct role for CBX4 in the DDR pathway.**

## INTRODUCTION

The cellular response to DNA double-strand breaks (DSBs) involves a plethora of proteins whose sequential recruitment and function at DNA damage sites are modulated by numerous highly dynamic and reversible post-translational modifications (1,2). These include phosphorylation, ubiquitylation, acetylation, methylation and sumoylation. The phosphorylation/dephosphorylation events are performed by kinases such as ATM, ATR and DNA-PK, and several protein phosphatases (1). The emerging ubiquitylation cascade comprises the E3 ubiquitin ligases RNF8, RNF168 and BMI1/RING-2, as well as the E2 ubiquitin-conjugating enzyme UBC13 (3–9). Unlike the classical role of ubiquitylation in triggering protein degradation, this ubiquitin-mediated pathway promotes genomic integrity by orchestrating protein–protein interactions on damaged chromosomes that allow recruitment of key DNA repair factors to DSBs, including 53BP1 and BRCA1 proteins, as reviewed in ref. (10–12).

Sumoylation has been implicated in the regulation of many processes, including transcriptional repression, genome stability, and chromatin organization, as reviewed in (13). In yeast, processes critical for cell fate decisions including survival and some aspects of DNA repair have been linked to sumoylation (14–16). Protein sumoylation is accomplished through a multitude of enzymes that, although mechanistically similar to ubiquitylation, utilize SUMO-specific enzymatic machinery (16,17). *In vitro* SUMO-1 modification requires two enzymatic steps, E1 and E2. Following cleavage of the SUMO-1 precursor, conjugation of SUMO-1 is accomplished by an enzymatic cascade employing E1 and E2 proteins that form an isopeptide bond between the ε-amino group of a lysine in the receptor protein and a C-terminal glycine in mature SUMO-1 (18–21). SUMO-1 activation by an E1 heterodimeric Aos1/Uba2 enzyme is followed by transfer of SUMO-1 to the conjugating E2 protein Ubc9. Several structurally unrelated SUMO E3 ligases have been identified that are required for efficient modification *in vivo* (16). These include proteins belonging to the protein inhibitor of activated STAT (PIAS) family, Ran-binding protein 2 (RanBP2) and CBX4, a PcG protein. All E3 ligases

*To whom correspondence should be addressed. Tel: +1 780 432 8439; Fax: +1 780 432 8892; Email: mhendzel@ualberta.ca

interact with Ubc9 and SUMO, which increases the rate of substrate sumoylation. The ability of CBX4 to function as a SUMO E3 ligase depends on a C-terminal substrate binding domain and an N-terminal region containing the chromodomain (22). All SUMO E3s are self-sumoylated and each localize to distinct subnuclear structures (23). PIAS1/4 is partly concentrated in subnuclear bodies, whereas RanBP2 associates with the nuclear pore complex, and CBX4 is found in nuclear foci called PcG bodies (16,22,24–26).

PcG bodies, which contain Polycomb repressive complexes, were originally identified in *Drosophila melanogaster* as regulators of homeotic gene expression and play important roles in the epigenetic maintenance of the repressed transcriptional state of genes (27). PcG members are chromatin-associated proteins that initiate and maintain heritable gene repression patterns (11,27,28). They are important for embryonic and adult stem cell self-renewal and maintenance, acting partially through repression of the INK4a/ARF locus. Aberrant silencing of this and other tumour suppressor loci by PcG-related mechanisms are now implicated in cancer development, as reviewed in (28). At least two distinct human PcG complexes have been identified. Polycomb repressive complex I (PRC1) contains CBX4/Pc2, HPH1 and RING domain-containing proteins (RING1, RING-2 and BMI1) (3). The core components of Polycomb repressive complex II (PRC2) include EED, SUZ12 and the SET-domain-containing histone methyltransferase EZH2. Three distinct enzymatic activities have been linked to these PcG complexes: sumoylation, ubiquitylation, and methylation (11).

Despite the critical role of sumoylation for survival in yeast following DNA damage, the direct involvement of sumoylation in the DSB response and its functional interplay with the ubiquitylation cascade was only recently demonstrated in mammals (29,30). These studies provide evidence of a key role for sumoylation in coordinating the DDR. They demonstrated that the E3 SUMO ligases PIAS1 and PIAS4 rapidly accumulate at the sites of DNA damage and that PIAS1 and PIAS4 are required for DSB-induced ubiquitylation mediated by the RNF8 and RNF168 ubiquitin ligases, whose activities are essential for efficient recruitment of the downstream factors 53BP1 and BRCA1 at DNA damage sites (29,30). It remains unclear whether PIAS1 and PIAS4 were the only E3 SUMO ligases involved in the DDR or if other E3 SUMO ligases coordinate aspects of the DDR. Here, we identify CBX4 as an early DDR protein that critically regulates the cellular response to DSBs. CBX4 SUMO activity is required for the recruitment of BMI1 to DNA damage sites, thereby initiating the BMI1-dependent DDR ubiquitylation pathway that provides radiation resistance to cells independent of RNF8 or H2AX.

## MATERIALS AND METHODS

### Cell culture, vector construct and transfections

Human embryonic kidney 293 cells (HEK 293) were cultured (air/CO2, 19:1, 37°C) in DMEM medium supplemented with 10% foetal bovine serum (Hyclone-ThermoFisher Scientific, Ottawa, Canada). Penicillin (100 U/ml) and streptomycin (100 mg/ml) (Wisent, St-Bruno, Canada) were added to culture media. A human mCherry-PARG-mut expressing vector was prepared by oligonucleotide-directed mutagenesis of the GFP-hPARG-110 (pEGFP-C1 expression vector, Clontech) as described in (31). Mutagenic primers were made following the guidelines in the QuikChange® site-directed mutagenesis kit (Stratagene). A mutation was introduced at amino acid position 756 that completely abolish PARG catalytic activity (E756D), as reported in (32). Wild-type and mutagenized PARG cDNAs were transferred into pmCherry-C1 vector (Clontech). Human YFP-CBX4 chromodomain and chromobox CBX4 mutants were generously provided by Dr. Tom Kerppola. Control and two different CBX4 shRNA plasmids were obtained from Origene. Smart pool non-GFP-labelled CBX4 siRNAs were also used (Dharmcon). For PIAS1 or PIAS4 shRNA, a previously described shRNA against PIAS1 or against PIAS4 was cloned into separate eGFP vectors (29) using the exact shRNA service at Origene. All shRNA transfections were performed with 0.2 μg DNA using Effectene as a transfection reagent (Qiagen) according to the manufacturer's instructions. All deletion mutants were generated by using the QuikChange site-directed mutagenesis kit (Stratagene). Purified proteins were either purchased from Boston Biochem or Abnova. U2OS cells were cultured in Mycos 5A medium containing 10% foetal calf serum (FCS) at 37°C and 5% $CO_2$. RNF8 WT and RNF KO (Dr. Xiaochun Yu), BMI1 WT and BMI1 KO (Dr. Maarten van Lohuizen) and H2AX wild-type and H2AX knockout mouse embryonic fibroblasts (André Nussenzweig) were grown in DMEM supplemented with 10% FCS. Several human cell cultures were included in this study to examine the potential contributions that ATM and DNA-$PK_{CS}$ may have in the recruitment of CBX4 to DNA break sites. These cell lines were propagated in DMEM/F12 (1:1) containing 10% FBS supplemented with 1 mM glutamine. The pEBS7 (EBS) and pEBS7-YZ5 (YZ5) cells are SV40-transformed cells from a single AT-patient where EBS are ATM defective whereas YZ5 stably express full-length ATM and are therefore isogenic (33). Finally, M059J (lacks DNA-$PK_{CS}$) and M059K (control) cells were derived from a malignant glioma isolated from a single human patient (34). Unless otherwise stated, cells were irradiated in ambient air using a model CS-600 $^{137}Cs$ irradiator (Picker, Glendale, CA) at a dose rate of 1 Gy/min.

### Immunofluorescence microscopy

Immunofluorescence was carried out as previously reported (3). A panel of commercially available primary antibodies, directed against various DNA damage proteins and Polycomb group proteins [BMI1 (Bethyl), PAR (Abcam), CBX4 (Novus), CBX4 (Millipore), SUMO-1 (Abcam), SUMO-2 and SUMO-3 (Abcam), 53BP-1(Lake Placid), MDC1 (Abcam) and PAR

(Calbiochem)] were used to detect proteins at sites of DNA damage.

### Two-photon micro-irradiation

Cells grown on coverslips were incubated with 0.5 μg/ml Hoechst 33258 for 15 min and then placed on the stage of a Zeiss LSM510 NLO laser-scanning confocal microscope. DSBs were generated as previously described (3) using a near-infrared 750 nm titanium-sapphire laser line. The laser output was set to 5–10% (unless stated otherwise), and we used 10 iterations to generate localized DSBs with a Plan-Neofluar 40×/1.3 N.A. oil immersion objective. For immunofluorescence staining of micro-irradiated cells, cells were permitted to recover in a 37°C humidified incubator containing 5% $CO_2$ for the indicated times post damage before 4% paraformaldehyde fixation and indirect immunofluorescent staining as detailed above. The average accumulation ± SE of fluorescently tagged proteins from at least 15 cells each from three independent experiments was plotted.

### Nuclear extractions and immunoblotting

Nuclear extraction and immunoblotting was performed as previously described (3). Secondary antibodies were conjugated with infrared specific dyes (either Alexa Fluor® 680 or Alexa Fluor® 750 or IRDye® 800), and fluorescence was imaged on the Odyssey Infrared Imaging system (LiCor Biosciences).

### Immunoprecipitation of YFP-CBX4

Cells were seeded onto 150-mm cell culture dishes and grown up to 80–90% confluency (~15–20 millions cells/dish). Experiments were performed with cell extracts from three dishes per condition. GFP (control) and YFP-CBX4 transfections were carried out with Effectene (Qiagen), as recommended by the manufacturer, and cells were harvested 16 h post-transfection. All further steps were performed on ice or at 4°C. Two PBS washes were carried out prior to protein extraction with 3 ml/plates of lysis buffer [40 mM HEPES, pH 7.5, 120 mM NaCl, 0.3% CHAPS, 1 mM EDTA, 1× Complete™ protease inhibitor cocktail (Roche Applied Science, Indianapolis, IN) and 1 μM PARG inhibitor ADP-HPD]. Total cell lysates were pooled and placed on ice for 15 min and gently mixed for another 15–20 min on a rotating device for complete lysis. After homogenization, insoluble material was removed from the homogenate by centrifugation at 5000 rpm for 5 min. Immunoprecipitation experiments were performed using Dynabeads™ magnetic beads covalently coupled to Protein G (Invitrogen, Burlington, Canada). The Dynabeads™ (100 μl/condition) were washed two times with 1 ml of 0.1 M sodium acetate buffer, pH 5.0, and coated with mouse monoclonal anti-GFP antibody (Roche Applied Science). The beads were washed three times with 1 ml of lysis buffer and added to the protein extract for 2 h incubation with gentle mixing on a rotating device. Samples were washed three times with 10 ml of lysis buffer for 5 min. Protein complexes were eluted using 150 μl of 3X Laemmli sample buffer containing 5% β-mercaptoethanol and heated at 65°C for 5 min in a water bath.

### Polymer-blot assays

Immunoprecipitated proteins from nuclear extracts were resolved using 4–12% Criterion™ XT Bis-Tris gradient gel (Bio-Rad) and transferred onto 0.2 μm nitrocellulose membrane. Bovine serum albumin (BSA) (Sigma) and core histones purified from HeLa chromatin by hydroxylapatite column chromatography (Active motif) were used as negative and positive PAR-binding controls, respectively. The proteins were partly renatured by incubating the membrane for 1 h at room temperature with gentle agitation in TBS-T (10 mM Tris-HCl, pH 8.0, 150 mM NaCl, 0.1% Tween-20) with frequent washes with TBS-T. Then, the membrane was incubated 1 h with TBS-T containing 250 nM of $^{32}$P-labelled pADPr purified on dihydroxyboryl Bio-Rex (DHBB) resin as described previously (35). The membrane was washed with the TBS-T buffer until no radioactivity could be detected. The membrane was subsequently air-dried and subjected to autoradiography on Bio-Max (Kodak) films.

### *In vitro* sumoylation assay

*In vitro* sumoylation reactions were performed using purified recombinant proteins according to a previously described procedure (22) with some modifications. The reaction mixtures (20 μl each) contained 50 mM Tris/HCl, pH 7.5, 5 mM $MgCl_2$, 2 mM ATP, 250 ng of Aos1/Uba2, 100 ng of Ubc9, 2 μg of SUMO-1, 400 ng of GST-BMI1 and 500 ng of CBX4. Reactions were carried out at 30°C for 2 h and terminated by the addition of SDS loading buffer. Products were analyzed by SDS/PAGE and immunoblotting.

### Colony formation assay for IR sensitivity

IR sensitivity was assayed using the colony formation assay as described previously (36). In brief, cells were left to grow for 10 days. After 10 cells, the cultures were fixed and stained with crystal violet, and then colonies were counted. Error bars are from duplicate samples.

### Chromatin immunoprecipitation assays

For Chromatin immunoprecipitation (ChIP) analysis, induction of a single DSB in MCF7 cells was performed as previously described (37) with the following modifications. MCF7 cells were transfected with pYFP-CBX4 and electroporated 18 h later with the I-*Sce*I expression vector pCBASce using the Gene Pulser Xcell apparatus (BioRad). ChIPs were performed as described (37), except that cells were sonicated for 10 × 30 s to shear chromatin to an average size of 0.5 kb using a Bioruptor (Diagenode). Immunoprecipitations were conducted with a monoclonal anti-GFP (Roche, cat 11 814 460 001) and a control mouse IgG (Jackson Immunoresearch). Quantification of the amount of immunoprecipitated DNA was carried out by real-time PCR using the LightCycler Fast Start DNA Master SYBR Green I (Roche Applied Sciences), which contained

Fast Start *Taq* DNA polymerase and SYBR Green Dye. The sequence of the primers can be obtained on request. Primers used in the PCR reactions were analyzed for linearity range and efficiency using a LightCycler (Roche). The results are presented as percentage of input for the IgG control versus the CBX4 immunoprecipitate.

## RESULTS

### CBX4 is an early DDR protein

We and several other groups have recently shown that members of the PRC1 complex, BMI1 and RING2, are recruited to sites of DNA damage where they ubiquitylate the histone H2A, initiating an H2AX- and RNF8-independent ubiquitylation cascade that is required for genomic integrity (3,4,38,39). It has been shown that PIAS1 and PIAS4 act in parallel but overlapping SUMO-conjugation pathways to promote RNF8-dependent ubiquitin adduct accumulation at the sites of DNA damage. CBX4 is a member of the PRC1 complex, and it was recently shown that, in response to DNA damage, HIPK2 regulates the E3 SUMO activity of CBX4 towards itself (40). This prompted us to examine whether, similar to RNF8-dependent ubiquitylation pathway, the Polycomb pathway is also regulated by sumoylation. Proteins with roles in the sensing and repair of DNA damage often localize to the surrounding chromatin (1). To investigate the role of CBX4 in the DDR, human bone osteosarcoma cells (U2OS) in the presence or absence of ionizing radiation (IR) treatment were subjected to immunostaining and CBX4 localization was examined. Notably, we found that, while CBX4 concentrated in several defined domains, PcG bodies, in untreated human cells (Supplementary Figure S1), 30 min after IR treatment, it formed nuclear foci that largely co-localized with γ-H2AX, suggesting them to be ionizing radiation (IR)-induced foci (IRIF) (Figure 1A). Similar co-localization patterns were established with BMI1, another PcG protein that has recently been implicated in the DDR (3,4,36,41–43) (Figure 1B). We confirmed these results using 750 nm two-photon laser micro-irradiation, which revealed that CBX4 localized to laser-induced DNA damage sites that overlap with γ-H2AX (Supplementary Figure S2). This treatment resulted in rapid recruitment of YFP-CBX4 to DNA damage tracks in live cells (Figure 1C). We found that CBX4 accumulated at irradiated sites within 11 s after micro-irradiation. Since the kinetics of CBX4 recruitment

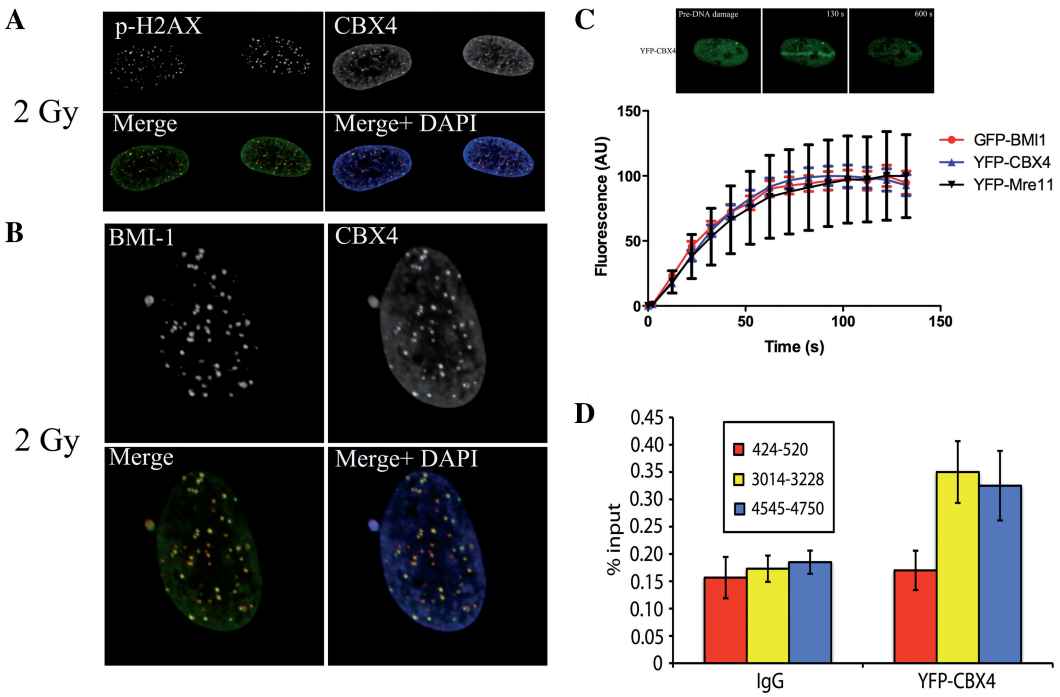


**Figure 1.** CBX4 is an early DDR protein. (**A**) U2OS cells were exposed to 2 Gy of radiation. Cells were permeabilized with 0.2% Triton-X100 in PBS, fixed and stained with (**A**) CBX4 and γ-H2AX antibodies or (**B**) BMI1 and CBX4 antibodies. Images were deconvolved with a constrained iterative deconvolution using a theoretical point spread function using Huygens Essential deconvolution software (Scientific Volume Imaging). (**C**) Kinetics of CBX4 in living cells. U2OS cells expressing YFP-CBX4, GFP-BMI1 or YFP-Mre11 were monitored after micro-irradiation by time-lapse fluorescence microscopy. Representative images of CBX4 time lapse are shown (top). The scale bar represents 5 μm. Quantification of YFP-CBX4, GFP-BMI1 and YFP-Mre11 accumulation at laser track sites was done using the Zeiss LSM software. The fluorescence intensity values in the micro-irradiated areas were pooled from 10 to 15 independent cells and plotted versus time (bottom). Experiment was done three times. (**D**) Detection of CBX4 on a unique DSB *in vivo* at a high resolution by chromatin immunoprecipitation (ChIP). Real-time PCR on ChIP samples was carried out at 191–335, 3014–3228 and 4545–4750 nucleotides from the break (red, yellow and blue bars, respectively). The average percentage of input for IgG and YFP-CBX4 at the GAPDH control locus is 0.23% and 0.22%, respectively. The data were generated from three independent experiments and eight PCR values from these experiments.

to the sites of DNA damage is similar to early DDR proteins such as MRE11 and BMI1 (3) (Figure 1C), these data suggest that the Polycomb E3 SUMO ligase CBX4 is one of the early factors involved in the DDR. CBX4 accumulation at the sites of DNA damage was not cell type specific. We observed CBX4 recruitment in a panel of cell lines ranging from mouse to human (Supplementary Figure S2). Consistent with our data, a recent report showed that CBX4 accumulated at the sites of UV laser induced DNA damage (38). However, in the previous work, it was unclear what signal CBX4 was responding to because UV laser irradiation induces multiple types of DNA lesions such as base damage, single-strand breaks and DSBs. Our demonstration that CBX4 accumulates at foci in response to irradiation (IRIF) suggests that CBX4 is responding to DSBs, although we cannot rule out that other types of damage also participate in the recruitment to sites of laser micro-irradiation.

In order to determine whether CBX4 binds very close to DSBs *in vivo* or is associated with flanking chromatin, we used ChIPs. For this, we employed the MCF7 cell line, which bears a modified GFP gene in which an I-*Sce*I restriction site has been engineered (37). The I-*Sce*I restriction enzyme does not cut elsewhere in the genome and therefore is specific for the modified GFP. In this way, a unique DSB can be created in a known nucleotide sequence. Following transfection of MCF7 cells with pCBASce (a plasmid encoding I-*Sce*I), a unique focus was present in 40% of the cells, compared to untransfected cells, as monitored by immunofluorescence with γ-H2AX (data not shown). Early after transfection with pCBASce, cells transfected with YFP-CBX4 were fixed with formaldehyde and the chromatin was solubilized by sonication and purified. Immunoprecipitation was performed with an antibody raised against GFP, which is also efficiently recognizing the YFP tag. Mouse anti-human IgG (H+L) antibody was used as a negative control. Control experiments revealed that GFP antibody immunoprecipitated YFP-CBX4 from the isolated chromatin (Supplementary Figure S3). After reversal of the formaldehyde crosslinks, DNA samples were deproteinized. DNA was isolated and amplified by real-time PCR with primer pairs specific to regions of interest near the DSB created by I-*Sce*I. All reactions were normalized against control primer pairs for sequences near the GAPDH locus, which allowed us to control for DSB-independent effects on protein occupancy. This highly informative approach allowed the detection of repair proteins on the DSB (37). We found that CBX4 was enriched (~2-fold) at 3 kb and 4.5 kb from the break site (Figure 1D).

### Mapping of the domains required to target CBX4 to DNA damage sites

To define the domain(s) that are responsible for CBX4 recruitment, we employed a series of YFP-tagged CBX4 deletion mutants (Figure 2A). CBX4 contains two previously characterized functional domains (44). The N-terminal region contains a highly conserved chromodomain (Chr), which binds to H3K9me3 and H3K27me3 residues. Also, CBX4 has a conserved region of 21 amino acids comprising the Pc box of CBX4 (Box) that is involved in transcriptional silencing and binding to other PcG proteins. The mutations in CBX4 used include ΔChr, deletion of the CBX4 chromodomain; ΔBox, deletion of the CBX4 chromobox; and ΔChr ΔBox, combined deletion of both CBX4 domains. We also introduced a single amino acid substitution of the CBX4 chromodomain (I16F) that is required to bind to the trimethylated lysine peptide on H3 and has been shown to reduce association of CBX4 with chromatin (44). YFP-tagged WT or mutant CBX4 constructs were transfected into U2OS, and the recruitment of CBX4 to the sites of DNA damage was examined by time-lapse microscopy. Western blot analysis using extracts from YFP-CBX4 expressing U2OS cells revealed that the level of expression of each CBX4 expression construct is very similar (Figure 2B). Introduction of the I16F point mutation, which eliminates trimethylation-dependent binding to the histone H3 N-terminus, had no significant effect on CBX4 recruitment to the sites of DNA damage (Figure 2C). Similarly, neither deletion of the chromodomain nor deletion of the chromobox abrogated recruitment to DNA damage sites (Figure 2C). Nonetheless, deletion of both domains, while not eliminating recruitment, significantly reduced recruitment. These data indicate that the mechanism of CBX4 recruitment to sites of DNA damage is distinct from those used to execute its PcG gene silencing function, where the chromodomain binds to H3K27me3 residues.

### PARP activity is required for CBX4 recruitment to DNA damage sites

To delineate where CBX4 fits in the established DNA damage-signalling cascade, we examined CBX4 recruitment in a number of human or mouse cells with deficiencies in various DNA damage response proteins. Cells were micro-irradiated using a 750 nm laser, and the micro-irradiated sites were examined by indirect immunofluorescence. Strikingly, we found that CBX4 accumulation at sites of laser-induced DNA damage is not significantly affected in cells with H2AX, ATM, DNA-PKcs, RNF8, 53BP1, Ku80 or HIPK2 deficiency (Supplementary Figures S4 and S5). We found no significant difference in either the recruitment kinetics or the retention of YFP-CBX4 in any of the cell lines tested (Figure 3B–E). These data suggest that the mechanism(s) responsible for recruiting CBX4 to DNA damage sites is distinct from previously established pathways. Since H2AX and numerous early DDR factors had no role in CBX4 recruitment, we initiated a search for alternative pathways that could be responsible for CBX4 recruitment. We focused our attention on poly(ADP-ribosyl)ation since this post-translational modification is known to have profound impacts on chromatin structure and genome functions (45) and has been reported to be involved in the recruitment of PcG proteins to sites of laser-induced DNA damage (38). Following genotoxic insult, DNA-dependent PARPs rapidly synthesize an

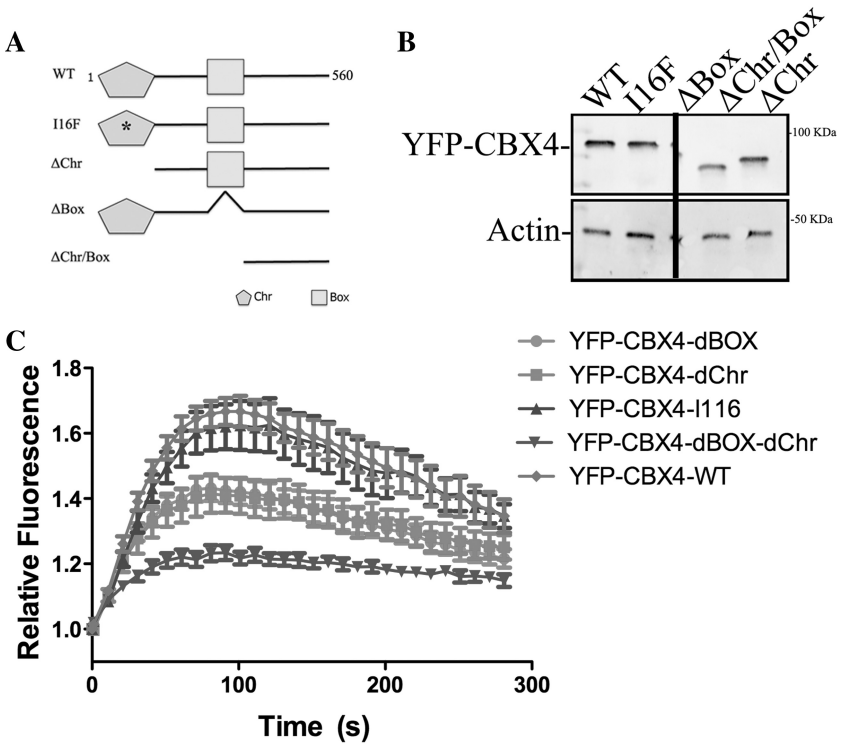


**Figure 2.** Mapping out the CBX4 domain(s) required for accumulation at sites of DNA damage. (**A**) Schematic diagrams for the CBX4 deletion mutants used. (**B**) Western blot analysis of U2OS cells expressing each of the CBX4 mutants to show the expression level of each mutant. (**C**) Quantitative time-lapse analysis of the effects of conserved CBX4 domains on CBX4 recruitment to the sites of DNA damage. WT, wild type; I16F, point mutation in the CBX4 chromodomain; ΔChr, deletion of the CBX4 chromodomain; ΔBox, deletion of the CBX4 chromobox; ΔChr ΔBox, combined deletion of both CBX4 domains. Quantifications of YFP-CBX4 deletion mutant accumulation at the laser track sites were done using the LSM software. The fluorescence intensity values in the micro-irradiated areas were pooled from 10 to 15 independent cells from three independent experiments and plotted on a time scale. The black line indicates that the intervening lanes were spliced out.

anionic poly(ADP-ribose) matrix that triggers local chromatin relaxation while acting as a loading platform for a variety of DDR factors (46). Poly(ADP-ribosyl)ation reactions are typically brief and transient phenomena due to the rapid hydrolysis of PAR by the poly(ADP-ribose) glycohydrolase (PARG) (47). To explore a role for PAR-metabolizing enzymes in the recruitment of CBX4 to sites of DNA damage, we asked whether a broad spectrum PARP inhibitor (AG-14361) could affect CBX4 accumulation dynamics. U2OS cells stably expressing YFP-CBX4 were pre-treated with either DMSO (control) or PARP inhibitor (AG-14361) for 1 h before 750-nm laser micro-irradiation, and the recruitment of YFP-CBX4 to the sites of DNA damage was monitored using time-lapse microscopy. CBX4 was recruited efficiently to DNA lesions in control-treated cells, but recruitment was largely abrogated in cells treated with the PARP inhibitor (Figure 3A). To further evaluate the role of PAR polymer in CBX4 recruitment to the sites of DNA damage, mCherry-tagged PARG constructs were used to modulate nuclear PAR levels (48). The expression of a wild-type (PARG-WT) and catalytically inactive (PARG-mut) 111-kDa nuclear PARG isoforms was used to modulate PAR turnover and assess whether PAR levels can have an impact on CBX4 recruitment (48). U2OS cells were co-transfected with mCherry PARG-WT or PARG-mut constructs together with YFP-CBX4, and the recruitment of YFP-CBX4 to the sites of DNA damage was monitored using time-lapse microscopy. We found that overexpression of PARG-mut did not have an impact of CBX4 recruitment to the DNA damage sites, whereas overexpression of PARG-WT abrogated the recruitment of CBX4 to the DNA damage sites (Figure 3B).

### CBX4 binds to PAR *in vitro*

The requirement for PAR chains to recruit CBX4 raised the possibility that CBX4 might bind PAR polymer chains directly. To test this hypothesis, YFP-CBX4 was transfected into HEK293 and affinity-purified using anti-GFP antibodies coupled to magnetic Protein-G Dynadeads. YFP differs from GFP due to a mutation at T203Y; antibodies raised against full-length GFP should also detect YFP and other variants. CBX4 immunoprecipitations were performed under normal growth conditions (untreated cells) or following massive PARP activation by the DNA alkylating agent MNNG. The immunoprecipitated proteins were resolved by SDS-PAGE and stained with SYPRO. YFP-CBX4 was highly enriched as shown by the prominent 100-kDa band revealed by the staining (Figure 3C). However, we failed to observe a typical YFP-CBX4 band shift in MNNG-treated cells that would suggest that CBX4 is directly covalently poly(ADP-ribosyl)ated by PARP-1. However, when the

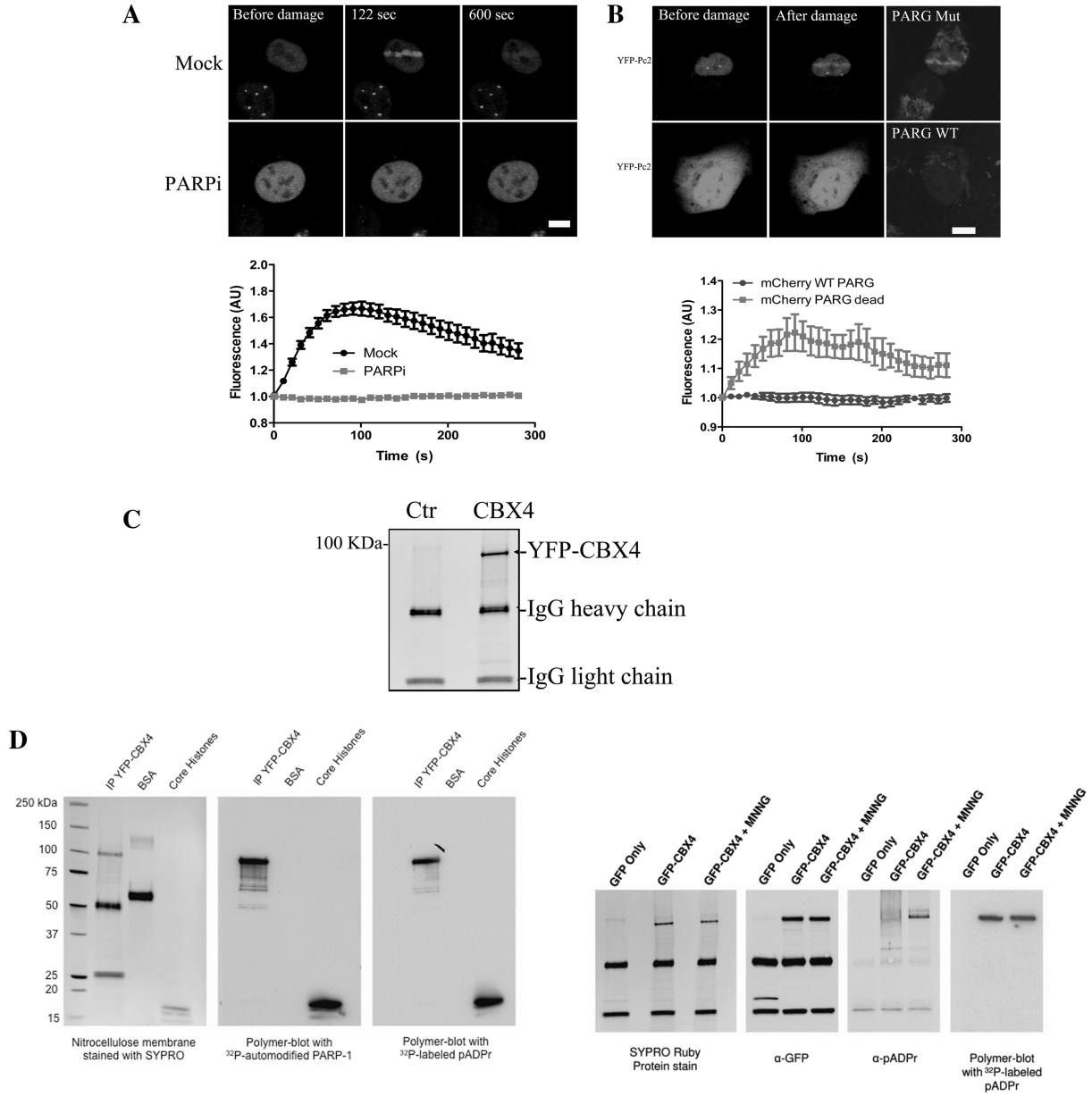


**Figure 3.** PARP mediates CBX4 recruitment to DNA break sites. (**A**) Effect of PARP inhibitor (PARPi) on CBX4 recruitment to the sites of DNA damage. U2OS cells were treated with PARPi (2.5 μM) for 1 h before DNA damage. DNA damage was introduced by laser micro-irradiation, and the recruitment of CBX4 to the sites of DNA damage was recorded. (**B**) Effect of PARG WT and PARG dead on CBX4 recruitment. mCherry-tagged PARG WT or PARG-mut were co-transfected with YFP-CBX4 into U2OS. Cells co-expressing YFP and mCherry were micro-irradiated, and the accumulation of CBX4 at the sites of DNA damage was recorded. The scale bar represents 5 μm. (**C**) YFP-CBX4 was transfected into HEK 293 cells and affinity-purified using anti-GFP antibodies coupled to magnetic Protein-G Dynadeads. The immunoprecipitated proteins were resolved by SDS-PAGE and stained with SYPRO. (**D**) Polymer blot of proteins immunoprecipitated with GFP antibody from nuclear extracts of cells expressing YFP-CBX4. Immunoprecipitated proteins were resolved by SDS-PAGE and stained with SYPRO (left), (middle left panel) incubated with $^{32}$P automodified PARP-1 and (right left panel) incubated with $^{32}$P automodified PAR. The identity of the PAR-binding signal on the blot was confirmed by immunodetection using anti-GFP and anti-CBX4 antibodies (right panels). BSA was used as a negative control for non-specific binding while purified core histones were used as positive control proteins for noncovalent PAR-binding.

immunoprecipitate was resolved by SDS-PAGE, transferred to nitrocellulose, and probed for proteins that bind PAR, strong noncovalent binding affinity for PAR was observed in the position of the gel where CBX4-YFP migrated (Figure 3D). The identity of the PAR-binding signal on the blot was confirmed by western blots using anti-GFP and anti-CBX4 antibodies (Figure 3E). The specificity of CBX4 binding to PAR was further examined on additional polymer blots (Figure 3D). BSA was used as a negative control to test nonspecific binding in our assay, whereas purified core histones were used as positive control proteins for non-covalent PAR-binding. Abundant proteins such as IgGs or the YFP tag itself did not bind PAR, and under the same conditions, BSA did not bind to PAR, whereas core histones bound PAR as expected (Figure 3D).

The polymer-blot assays indicate that CBX4 has the ability to directly bind PAR polymers *in vitro*. Taken together our results suggest that DNA damage induces PAR polymer synthesis that acts as scaffolding matrix that serves to directly recruit CBX4 to the sites of DNA damage.

### CBX4 mediates the accumulation of SUMO conjugates at DSBs

Three SUMO isoforms: SUMO-1, SUMO-2 and SUMO-3 accumulate at DSB sites and form IRIF in mammalian cells (29,30). Therefore, we examined whether or not CBX4 knock down had an effect on the formation of DNA damage-induced SUMO-1, SUMO-2 or SUMO-3 IRIF. Due to similarities in sequence, SUMO-2 and SUMO-3 cannot be distinguished to date and are thus referred to as SUMO-2/3 (49). The effect of CBX4 knock down on SUMO-1 and SUMO2/3 IRIF formation was examined in U2OS cells transfected with one of two different CBX4 shRNA prior to radiation exposure (2 Gy). Irradiated cells that have normal expression of CBX4 efficiently form SUMO-1 and SUMO-2/3 IRIF with an average of 28 foci per cell (Figure 4A). In contrast, CBX4 knock down reduced the average number of SUMO-1 and SUMO-2/3 foci per cell to 8. These data suggest that CBX4 regulates the accumulation of SUMO-1 and SUMO-2/3 at the sites of DNA damage. In control experiments, we confirmed that CBX4 shRNA constructs that co-express a GFP reporter specifically depleted CBX4 levels in cells and CBX4 knock down had no effect on the global SUMO-1 or SUMO-2/3 levels in cells (Supplementary Figure S6 and data not shown). Previous reports showed that PIAS1 and PIAS4 mediate SUMO-1 and SUMO-2/3 accumulation at DSB sites in an RNF8-dependent manner (29,30). Therefore, we next examined if SUMO-1 and SUMO-2/3 accumulate in RNF8 KO MEFs. In order to test this, YFP-SUMO-1 and YFP-SUMO-2/3 were transfected into RNF8 WT and RNF8 KO cells and the accumulation of SUMO-1 and SUMO-2/3 at the sites of DNA damage were monitored by time-lapse microscopy. Consistent with previous reports, we found that SUMO-1 accumulation at

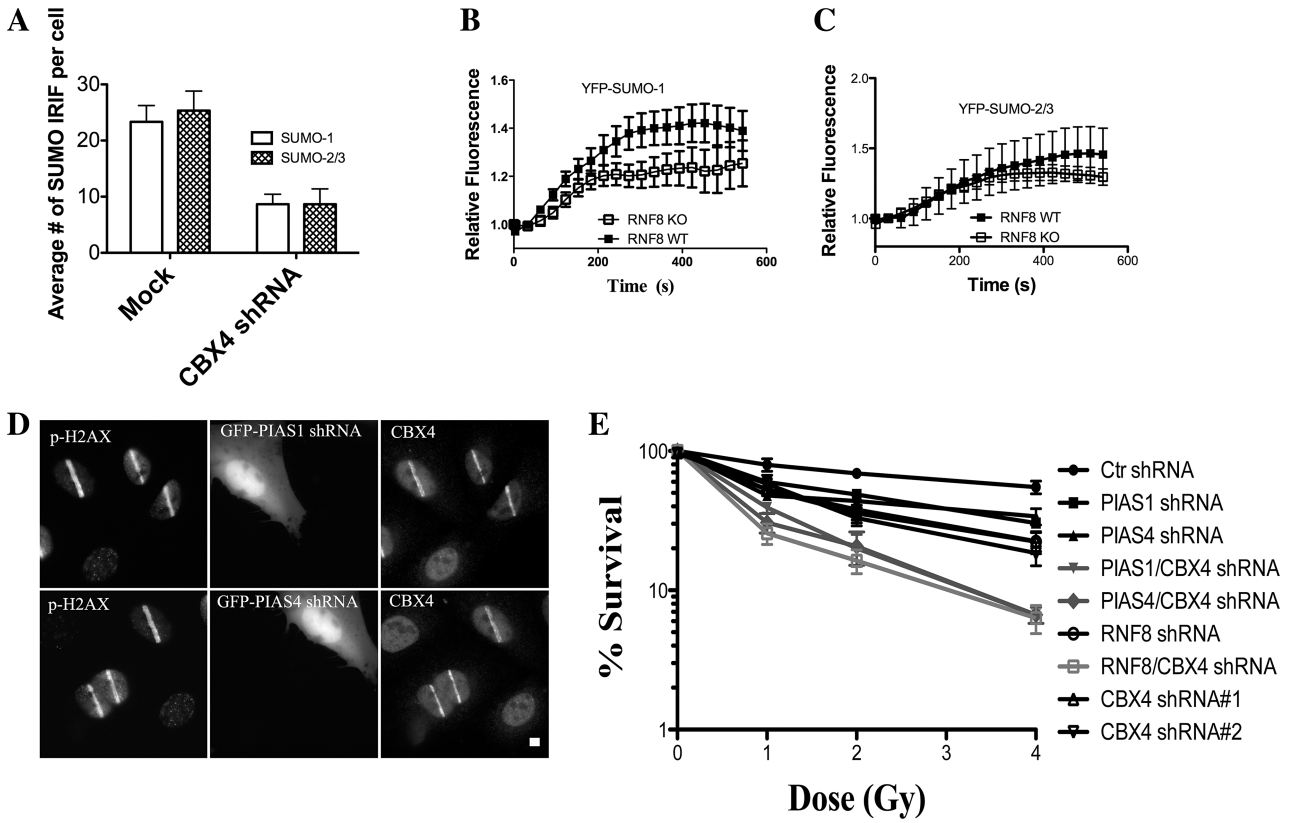


**Figure 4.** CBX4 and PIAS1/4-mediated DDR pathways are distinct. (**A**) Effect of CBX4 knock down (KD) on the formation of SUMO-1 and SUMO-2/3 IRIF. U2OS cells transiently expressing GFP-tagged CBX4 shRNA were exposed to 2 Gy of radiation; cells were fixed and co-immunostained with antibodies to SUMO-1 or SUMO-3 and γ-H2AX antibodies. An average number of SUMO-1 or SUMO-3 IRIF per cell were plotted. RNF8 WT and RNF8 KO MEFs transiently expressing either (**B**) YFP-SUMO-1 or (**C**) YFP-SUMO-3 were micro-irradiated, and the accumulation of SUMO was monitored by time-lapse fluorescence microscopy. The fluorescence intensity values in the micro-irradiated areas were pooled from 10 to 15 independent cells from three independent experiments and plotted on a time scale. (**D**) U2OS cells transfected with either PIAS1 shRNA construct or PIAS4 shRNA construct that co-expresses a GFP reporter were micro-irradiated, permitted to recover for 5 min at 37°C, and immunostained as indicated. The scale bar represents 5 μm. (**E**) CBX4 mediates resistance to radiation. Survival curves of U2OS cells transfected with either control shRNA or either one of two different CBX4 shRNA or double transfected with different shRNA as indicated, exposed to different doses of radiation and allowed to grow for 10 days. Cells were stained with crystal violet, and the number of remaining colonies was counted. The experiment was carried out in triplicate. Error bars represent standard error from three independent experiments.

laser-induced DNA damage was reduced but still readily detectable in RNF8 KO cells, indicating the existence of an RNF8-independant pathway that is responsible for the remaining SUMO-1 recruitment (Figure 4B and C) (29). In contrast, YFP-SUMO-2/3 accumulated efficiently in both RNF8 WT and RNF8 KO MEFs (Figure 4B and C) suggesting that SUMO-2/3 recruitment is RNF8 independent. Not surprisingly, CBX4 colocalized with SUMO-1, -2 and -3 at sites of DNA damage (Supplementary Figure S7).

### The PIAS1/PIAS4- and CBX4-mediated DNA damage response pathways are distinct

Recent reports identified PIAS1 and PIAS4 as E3 SUMO ligases that are required for SUMO-1 and SUMO-2/3 accumulation (29,30). Therefore, we wanted to determine whether or not the PIAS1, PIAS4 and CBX4 SUMO ligases function in the same or different DNA damage response pathways. A previously described shRNA against PIAS1 or against PIAS4 was cloned into separate eGFP vectors (29). PIAS1 or PIAS4 shRNAs constructs that co-express a GFP reporter were transfected into U2OS. Cells were subjected to laser micro-irradiation followed by immunofluorescence staining. We found that CBX4 accumulation at DNA damage sites was not affected by either PIAS1- or PIAS4-specific shRNA (Figure 4D). In a control experiment, these shRNA constructs efficiently knocked down the relevant protein in cells (Supplementary Figure S8). These data indicate that neither PIAS1 nor PIAS4 are required for the initial recruitment of CBX4 to DNA damage sites and suggest that PIAS1/PIAS4 and CBX4 function in distinct DDR pathways. To confirm whether or not CBX4 and PIAS1/PIAS4 were part of the same or distinct genetic pathways contributing to radiation resistance, the survival of either U2OS cells transfected with both PIAS1 or PIAS4 shRNA and CBX4 shRNA or U2OS cells transfected with both RNF8 shRNA and CBX4 shRNA was quantified. When challenged with moderate doses of IR (2 Gy), the transient knockdown of CBX4 significantly reduced the fraction of surviving cells (Figure 4E). The effect of CBX4 knockdown on cellular radiation sensitivity was more pronounced (3-fold) at 4 Gy. Interestingly, we found that knockdown of PIAS1 or PIAS4 together with CBX4 knockdown or simultaneous knockdown of RNF8 and CBX4 additively increased radiation sensitivity beyond the loss of either E3 ligase alone, implying that these E3 ligases are not part of the same genetic pathway (Figure 4E). Also, the sensitivity of cells to radiation upon CBX4 knockdown indicates a direct functional role for CBX4 in the DDR or repair of DNA damage.

### CBX4 is required for BMI1 recruitment to DSB sites

Since CBX4 contains the chromodomain that binds to trimethylated lysine 27 on histone H3 (H3K27me3) and thereby participates in targeting the Polycomb E3 ubiquitin ligase complex, PRC1, to genes undergoing repression, we tested the possibility that CBX4 is needed to target the PRC1 component, BMI1, to sites of DNA damage (50–52). BMI1 recruitment to DNA damage was examined in U2OS cells transfected with CBX4 shRNA construct that co-expresses a GFP reporter. Cells were exposed to 2 Gy of radiation, and the accumulation of BMI1 into IRIF was monitored. As a control, we counterstained cells with γ-H2AX antibody in order to reveal the sites of DNA damage (IRIF). Consistent with our previous observation (3), we found that BMI1 was enriched in IRIF that co-localize with γ-H2AX in U2OS cells having normal expression of CBX4 (3) (Figure 5A). In contrast, BMI1 accumulation at DSB sites was reduced in U2OS cells expressing GFP-CBX4 shRNA (Figure 5A). We then tested whether or not the recruitment of CBX4 and BMI1 to sites of DNA damage was mutually dependent on each other, which might occur because they coexist in the PRC1 complex. BMI1 wild-type (BMI1 WT) and BMI1 knock out (BMI1 KO) mouse embryonic fibroblasts (MEFs) (53) were micro-irradiated, and the recruitment of CBX4 was examined by indirect immunostaining. We found that CBX4 was efficiently recruited to the sites of DNA damage in both BMI1 WT and BMI1 KO MEFs (Figure 5B), demonstrating that CBX4 recruitment onto sites of DNA breaks is BMI1 independent. To further confirm these data, we examined the kinetics of CBX4 recruitment in BMI1 WT and BMI1 KO MEFs. Cells were transfected with full-length YFP-CBX4, and the kinetics of CBX4 recruitment to sites of DNA damage was monitored by time-lapse microscopy. We found no significant difference in either the recruitment kinetics or the retention of YFP-CBX4, when BMI1 WT is compared to BMI1 KO cells (Figure 5C). Taken together, these data suggest that CBX4 is essential for the accumulation of BMI1 at DSB sites, whereas CBX4 recruitment is independent of BMI1.

### DNA damage induces the sumoylation of BMI1 at lysine 88

The demonstration that CBX4 is required for targeting BMI1 to sites of DNA damage suggested the possibility that BMI1 is sumoylated in response to DNA damage. To directly test for BMI1 sumoylation, we transiently co-expressed myc-tagged-BMI1, Ubc9 and YFP-SUMO-1 and then performed myc immunoprecipitations. Immunoblotting of the resulting samples with an anti-BMI1 antibody established that, upon exposing cells to radiation, a slower migrating band was observed that is consistent with the conjugation of SUMO-1 to BMI1 (Figure 6A). This band was not present in cells not exposed to radiation suggesting that BMI1 is sumoylated in response to DNA damage. This conclusion is further supported by reciprocal GFP-immunoprecipitation western experiment. Indeed, anti-BMI1 immunoblotting confirmed that irradiation induced the sumoylation of BMI1 (Figure 6A). We next conducted computational analysis using the BMI1 primary sequence to predict potential BMI1 sumoylation sites. The analysis revealed one probable sumoylation site on BMI1, at lysine 88 (K88). To determine if lysine 88 is sumoylated, we created a version of BMI1 in which lysine 88 was mutated to arginine (K88R). BMI1 KO cells exposed or

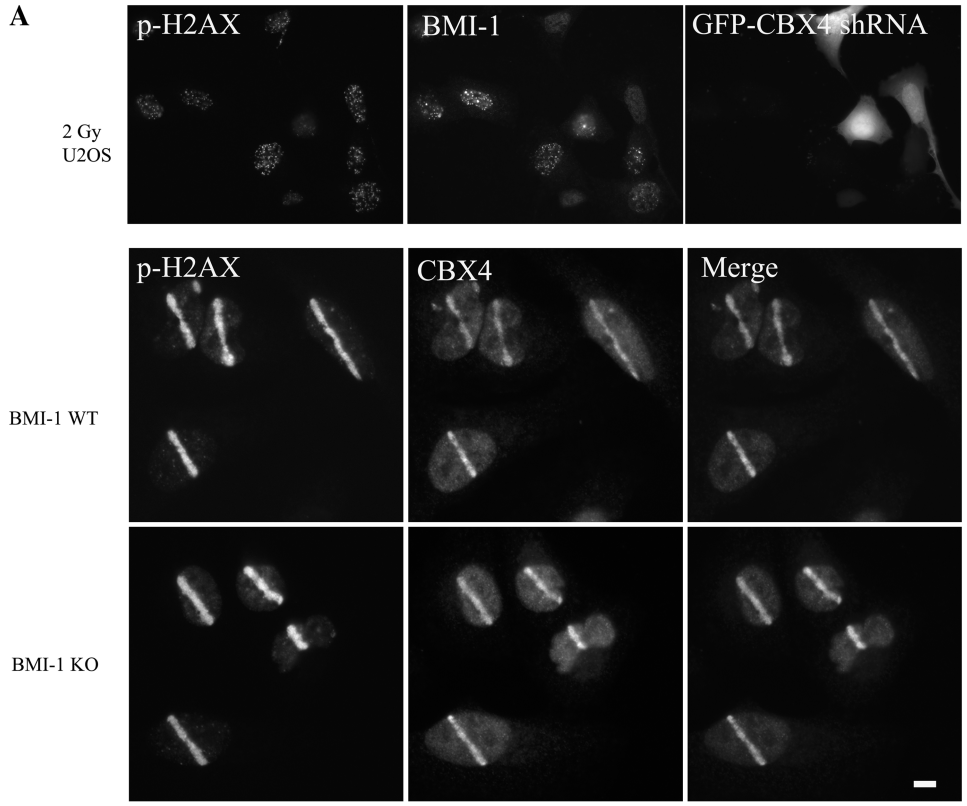


**Figure 5.** CBX4 is required for BMI1 localization to DNA damage sites. (**A**) U2OS cells transfected with CBX4 shRNA construct that co-expresses a GFP reporter were irradiated with 2 Gy and left to recover for 30 min at 37°C. Cells were fixed and immunostained for BMI1 and γ-H2AX. (**B**) BMI1 WT and BMI1 KO MEFs were micro-irradiated and left to recover for 5 min. Cells were fixed and stained as indicated. The scale bar represents 5 μm. (**C**) Dynamics of YFP-CBX4 in BMI1 WT and BMI1 KO MEFs. Cells were transfected with YFP-CBX4, and accumulation of YFP-CBX4 at the DNA damage sites was analyzed by time-lapse fluorescence microscopy. The fluorescence intensity values in the micro-irradiated areas were pooled from 10 to 15 independent cells from three independent experiments and plotted on a time scale.

not exposed to radiation were co-transfected with Ubc9, SUMO-1 and either GFP-BMI1 WT or GFP-BMI1 K88R and analyzed by western blot. Consistent with previous results, we found that DNA damage-induced sumoylation of BMI1 in cells reconstituted with the WT BMI1 construct (Figure 6B). Importantly, mutation of this lysine residue to arginine (BMI1 K88R) abrogated DNA damage-induced BMI1 SUMO modification *in vivo* (Figure 6B). We conclude that BMI1 is sumoylated in response to DNA damage and that lysine 88 is the principal lysine utilized for SUMO conjugation. We next studied the impact of K88R mutation on BMI1 recruitment to sites of DNA damage. U2OS cells were transfected with the GFP-BMI1 WT or GFP-BMI1 K88R construct, and the kinetics of BMI1 recruitment to sites of DNA damage was monitored by time-lapse microscopy. We found that K88R mutation severely reduced the recruitment of BMI1 to sites of laser-induced DNA lesions (Figure 6C). We conclude that lysine 88 is essential for BMI1 targeting to the sites of DNA breaks. To exclude that the mutation of K88 to R itself is responsible for the defect in BMI1 recruitment, independent of the

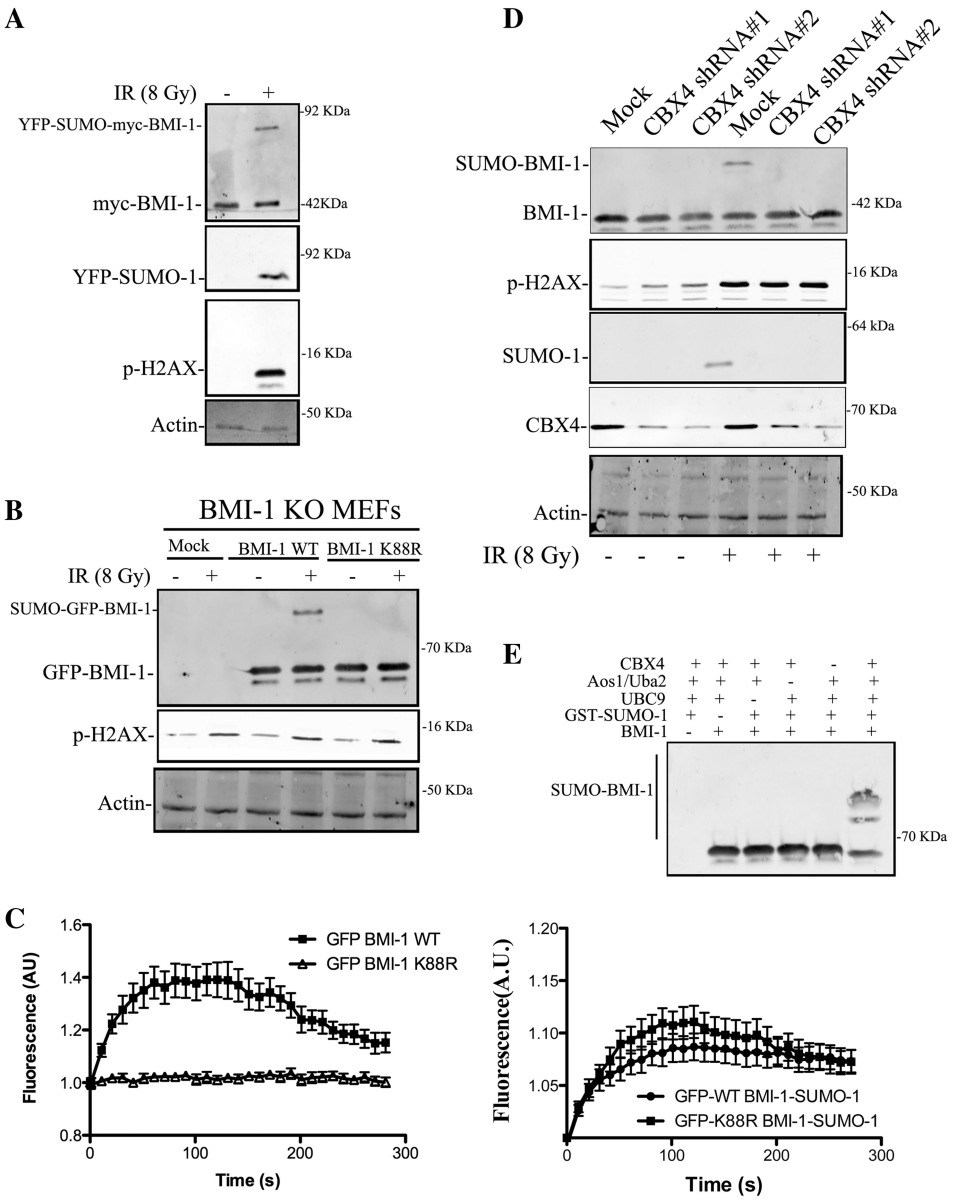


**Figure 6.** DNA damage-induced sumoylation of BMI1 at lysine 88. (**A**) 293T cells transiently transfected with CBX4, myc-tagged BMI1, Ubc9 and YFP-SUMO-1 were irradiated with 6 Gy and permitted to recover for 1 h at 37°C. Nuclear extracts were prepared and immunoprecipitated using myc or GFP-specific antibody. Immunoblot analysis was done using BMI1 antibody. As a control different blots were run simultaneously and probed with γ-H2AX and actin. (**B**) BMI1 KO MEFs reconstituted either with empty vector, GFP-BMI1 WT or GFP-BMI1 K88R constructs were treated as in (A). Nuclear extracts and immunoprecipitations were done using GFP antibody. Immunoblot analysis was done using BMI1 antibody. (**C**) Time-lapse fluorescence microscopy of GFP- WT BMI1, GFP- K88R-BMI1, GFP- WT-BMI1-SUMO1 or GFP-K88R-BMI1-SUMO-1 in U2OS following laser micro-irradiation. The fluorescence intensity values in the micro-irradiated areas were pooled from 10 to 15 independent cells from three independent experiments and plotted on a time scale. (**D**) U2OS cells expressing Ubc9 and SUMO-1 were transfected with either control or one of the two different CBX4, shRNA were irradiated with 6 Gy and permitted to recover for 1 h at 37°C. Nuclear extracts were immunoprecipitated and immunoblotted using BMI1 antibody. (**E**) CBX4 promotes SUMO-1 conjugation to BMI1 *in vitro*. Purified proteins GST-tagged BMI1 and GST-tagged CBX4 proteins were incubated with recombinant Aos1/Uba2 (E1), Ubc9 and SUMO-1 as indicated. The reaction mixture was analyzed by western blotting using anti-BMI1antibody.

sumoylation status, we constructed a fusion protein where SUMO-1 is attached to the C-terminus of either WT or K88R BMI1 and the recruitment of BMI1 to the sites of DNA damage was monitored. Interestingly, we found that fusing SUMO-1 to the K88R mutant abolished the recruitment defect observed with the K88R BMI1 construct, indicating that interactions mediated by SUMO are important in targeting BMI1 to DNA damage (Figure 6C).

### CBX4 mediates DNA damage-induced BMI1 sumoylation

We next wanted to examine if CBX4 is responsible for sumoylation of BMI1 in response to DNA damage. U2OS cells expressing Ubc9 and SUMO-1 were transfected with either control or one of the two different CBX4, shRNA were either mock treated or exposed to radiation and nuclear extracts were prepared.

Immunoblot analysis revealed that BMI1 was efficiently sumoylated in cells expressing control shRNA whereas CBX4 knock down completely abrogated DNA damage-induced BMI1 sumoylation (Figure 6D). To determine whether CBX4 can sumoylate BMI1 *in vitro*, purified GST-tagged BMI1 and GST-tagged CBX4 proteins were incubated with recombinant Aos1/Uba2 (E1), Ubc9 and SUMO-1 in the presence of ATP. Reactions were terminated by the addition of SDS-PAGE loading buffer and analyzed by western blot with a BMI1-specific antibody. When recombinant E1, Ubc9, CBX4 and SUMO-1 were all present, a slower migrating band was observed that is consistent with the conjugation of SUMO-1 to BMI1 (Figure 6E). This band was not present when E1, Ubc9, CBX4 or SUMO-1 was absent from the reaction mixture, demonstrating that CBX4 can sumoylate BMI1 *in vitro*. Taken together, these data suggest that CBX4 is required for the sumoylation of BMI1 in response to DNA damage.

## DISCUSSION

Protein sumoylation is an important post-translational modification, which can regulate multiple aspects of target protein function (54). Here we provide evidence that CBX4 is directly involved in the cellular response to DNA damage. We found that sumoylation of BMI1 by CBX4 affects its subcellular localization and is required for BMI1 recruitment to sites of DNA damage. CBX4-mediated sumoylation of BMI1 allows its recruitment to sites of DNA damage. This event initiates a novel ubiquitylation pathway that is required for radiation resistance and genomic integrity. CBX4 recruitment to the sites of DNA damage is independent of H2AX, RNF8, PI-3-kinase-related kinases and PIAS1/PIAS4, which distinguishes CBX4-dependent DDR signalling from other known pathways. The demonstration that CBX4 is recruited to the sites of DNA damage within seconds after damage and that CBX4 expression is necessary for cell survival upon exposure to irradiation leads to a model in which CBX4 plays an early critical role in the DDR. The newly discovered role of both SUMO and ubiquitin-based Polycomb-dependent signalling within the DDR cascade expands the role of PcG proteins beyond gene repression. Interestingly, the SUMO-mediated regulation of the Polycomb E3 ubiquitin ligase complex at sites of DNA damage illustrates that both the Polycomb pathway and the canonical RNF8 pathway use similar regulatory mechanisms. Recent reports implicated two E3 SUMO ligases PIAS1 and PIAS4 in the RNF8-dependent cellular response to DNA damage (29,30). The CBX4 SUMO ligase represents a distinct pathway since the recruitment of PIAS1 and PIAS4 to sites of DNA damage requires the E3 ubiquitin ligase RNF8 and the phosphorylation of H2AX, while CBX4 recruitment is independent of these factors. Additionally, CBX4 recruitment to sites of DNA damage is independent of PIAS1 and PIAS4. This suggests that PIAS1/PIAS4 and CBX4 are two independent SUMO pathways that operate within the DDR.

The PARP family of proteins has been implicated previously in the recruitment of DNA repair factors to lesions and is known to rapidly localize to sites of damage (46,55,56). PARP1, the best-characterized family member in mammalian cells, is involved in single-strand break repair and an alternative non-homologous end-joining pathway of DSB repair (38). The binding of PARP1 to DNA breaks stimulates its enzymatic activity and leads to the rapid assembly of PAR chains adjacent to the lesion. This assembly leads to the recruitment of X-ray repair cross-complementing group 1 and DNA ligase III, as well as polynucleotide kinase, polymerase-β, flap endonuclease-1, and PARP2 to the break site. Recently Chou *et al.* (2011) found that PARP activity was required for the accumulation of a number of PcG proteins at sites of DNA damage, including BMI1 and CBX4. Since they also found that EZH2 was recruited in a PARP-dependent manner, they proposed that there was a PARP-dependent recruitment PRC2 methyltransferase complex. Through the catalytic subunit, EZH2, PRC2 then recruited PRC1. However, we (11) and others (57) have not found increased histone H3 lysine 27 methylation at sites of DNA damage. In this light, our results implicate CBX4 as the component of PRC1 that is both responsible for the recruitment of the complex and directly interacts with poly(ADP-ribose). Two lines of evidence support such a scenario. First, CBX4 positive charge prediction identifies a domain in the N-terminus of CBX4 that has the potential to bind ribosylated polymer. Second, using polymer-blot assays we have shown that CBX4 has the ability to directly bind PAR polymers *in vitro*.

In conclusion, we present data that documents a new function for CBX4 within the DDR, further establishing the involvement of PcG in multiple cellular processes. The demonstration that CBX4 controls the sumoylation status of BMI1, and that this modification regulates BMI1 recruitment to sites of DNA damage in mammalian cells, establishes a new role for sumoylation in mediating interaction among PcG proteins.

## SUPPLEMENTARY DATA

Supplementary Data are available at NAR Online: Supplementary Figures 1–8.

## ACKNOWLEDGEMENTS

We thank Drs. Andre Nussenzweig, Xiaochun Yu, Maarten van Lohuizen, David Wotton and Tom Kerppola for providing valuable reagents. We also thank the Cellular Imaging Facility at the Cross Cancer Institute for the use of microscopes and image analysis software. We are grateful to Dr. Randall Gieni for critical reading of the manuscript.

## FUNDING

The Alberta Cancer Foundation (to M.H.) from the Alberta Cancer Foundation and the Canadian Institute

of Health Research (CIHR) (to G.P., M.H. and J.Y.M.); an Alberta Innovates Health Solutions (AIHS) Senior Scholar (to M.J.H.); and AIHS and Alberta Cancer Foundation postdoctoral fellowships (to I.H.I). Funding for open access charge: Alberta Cancer Foundation.

*Conflict of interest statement*. None declared.

## REFERENCES


1. Polo,S.E. and Jackson,S.P. (2011) Dynamics of DNA damage response proteins at DNA breaks: a focus on protein modifications. *Genes Dev*., **25**, 409–433.
2. Ismail,I.H. and Hendzel,M.J. (2008) The gamma-H2A.X: Is it just a surrogate marker of double-strand breaks or much more? *Environ. Mol. Mutagen*., **49**, 73–82.
3. Ismail,I.H., Andrin,C., McDonald,D. and Hendzel,M.J. (2010) BMI1-mediated histone ubiquitylation promotes DNA double-strand break repair. *J. Cell. Biol*., **191**, 45–60.
4. Ginjala,V., Nacerddine,K., Kulkarni,A., Oza,J., Hill,S.J., Yao,M., Citterio,E., van Lohuizen,M. and Ganesan,S. (2011) BMI1 is recruited to DNA breaks and contributes to DNA damage-induced H2A ubiquitination and repair. *Mol. Cell. Biol*., **31**, 1972–1982.
5. Kolas,N.K., Chapman,J.R., Nakada,S., Ylanko,J., Chahwan,R., Sweeney,F.D., Panier,S., Mendez,M., Wildenhain,J., Thomson,T.M. *et al*. (2007) Orchestration of the DNA-damage response by the RNF8 ubiquitin ligase. *Science*, **318**, 1637–1640.
6. Huen,M.S., Grant,R., Manke,I., Minn,K., Yu,X., Yaffe,M.B. and Chen,J. (2007) RNF8 transduces the DNA-damage signal via histone ubiquitylation and checkpoint protein assembly. *Cell*, **131**, 901–914.
7. Doil,C., Mailand,N., Bekker-Jensen,S., Menard,P., Larsen,D.H., Pepperkok,R., Ellenberg,J., Panier,S., Durocher,D., Bartek,J. *et al*. (2009) RNF168 binds and amplifies ubiquitin conjugates on damaged chromosomes to allow accumulation of repair proteins. *Cell*, **136**, 435–446.
8. Stewart,G.S., Panier,S., Townsend,K., Al-Hakim,A.K., Kolas,N.K., Miller,E.S., Nakada,S., Ylanko,J., Olivarius,S., Mendez,M. *et al*. (2009) The RIDDLE syndrome protein mediates a ubiquitin-dependent signaling cascade at sites of DNA damage. *Cell*, **136**, 420–434.
9. Mailand,N., Bekker-Jensen,S., Faustrup,H., Melander,F., Bartek,J., Lukas,C. and Lukas,J. (2007) RNF8 ubiquitylates histones at DNA double-strand breaks and promotes assembly of repair proteins. *Cell*, **131**, 887–900.
10. Al-Hakim,A., Escribano-Diaz,C., Landry,M.C., O'Donnell,L., Panier,S., Szilard,R.K. and Durocher,D. (2010) The ubiquitous role of ubiquitin in the DNA damage response. *DNA Repair*, **9**, 1229–1240.
11. Gieni,R.S., Ismail,I.H., Campbell,S. and Hendzel,M.J. (2011) Polycomb group proteins in the DNA damage response: a link between radiation resistance and "stemness". *Cell Cycle*, **10**, 883–894.
12. Panier,S. and Durocher,D. (2009) Regulatory ubiquitylation in response to DNA double-strand breaks. *DNA Repair*, **8**, 436–443.
13. Dou,H., Huang,C., Van Nguyen,T., Lu,L.S. and Yeh,E.T. (2011) SUMOylation and de-SUMOylation in response to DNA damage. *FEBS Lett*., **585**, 2891–2896.
14. Bergink,S. and Jentsch,S. (2009) Principles of ubiquitin and SUMO modifications in DNA repair. *Nature*, **458**, 461–467.
15. Branzei,D. and Foiani,M. (2008) Regulation of DNA repair throughout the cell cycle. *Nature Rev. Mol. Cell. Biol*., **9**, 297–308.
16. Hay,R.T. (2005) SUMO: a history of modification. *Mol. Cell*, **18**, 1–12.
17. Guo,B., Yang,S.H., Witty,J. and Sharrocks,A.D. (2007) Signalling pathways and the regulation of SUMO modification. *Biochem. Soc. Trans*., **35**, 1414–1418.
18. Desterro,J.M., Rodriguez,M.S., Kemp,G.D. and Hay,R.T. (1999) Identification of the enzyme required for activation of the small ubiquitin-like protein SUMO-1. *J. Biol. Chem*., **274**, 10618–10624.
19. Gong,L., Li,B., Millas,S. and Yeh,E.T. (1999) Molecular cloning and characterization of human AOS1 and UBA2, components of the sentrin-activating enzyme complex. *FEBS Lett*., **448**, 185–189.
20. Johnson,E.S., Schwienhorst,I., Dohmen,R.J. and Blobel,G. (1997) The ubiquitin-like protein Smt3p is activated for conjugation to other proteins by an Aos1p/Uba2p heterodimer. *EMBO J*., **16**, 5509–5519.
21. Okuma,T., Honda,R., Ichikawa,G., Tsumagari,N. and Yasuda,H. (1999) In vitro SUMO-1 modification requires two enzymatic steps, E1 and E2. *Biochem. Biophys. Res. Commun*., **254**, 693–698.
22. Kagey,M.H., Melhuish,T.A. and Wotton,D. (2003) The polycomb protein Pc2 is a SUMO E3. *Cell*, **113**, 127–137.
23. Bawa-Khalfe,T. and Yeh,E.T. (2010) SUMO losing balance: SUMO proteases disrupt SUMO homeostasis to facilitate cancer development and progression. *Genes Cancer*, **1**, 748–752.
24. Kotaja,N., Karvonen,U., Janne,O.A. and Palvimo,J.J. (2002) PIAS proteins modulate transcription factors by functioning as SUMO-1 ligases. *Mol. Cell. Biol*., **22**, 5222–5234.
25. Pichler,A., Gast,A., Seeler,J.S., Dejean,A. and Melchior,F. (2002) The nucleoporin RanBP2 has SUMO1 E3 ligase activity. *Cell*, **108**, 109–120.
26. Sachdev,S., Bruhn,L., Sieber,H., Pichler,A., Melchior,F. and Grosschedl,R. (2001) PIASy, a nuclear matrix-associated SUMO E3 ligase, represses LEF1 activity by sequestration into nuclear bodies. *Genes Dev*., **15**, 3088–3103.
27. Simon,J.A. and Tamkun,J.W. (2002) Programming off and on states in chromatin: mechanisms of Polycomb and trithorax group complexes. *Curr. Opin. Genet. Dev*., **12**, 210–218.
28. Gieni,R.S. and Hendzel,M.J. (2009) Polycomb group protein gene silencing, non-coding RNA, stem cells, and cancer. *Biochem Cell Biol*, **87**, 711–746.
29. Galanty,Y., Belotserkovskaya,R., Coates,J., Polo,S., Miller,K.M. and Jackson,S.P. (2009) Mammalian SUMO E3-ligases PIAS1 and PIAS4 promote responses to DNA double-strand breaks. *Nature*, **462**, 935–939.
30. Morris,J.R., Boutell,C., Keppler,M., Densham,R., Weekes,D., Alamshah,A., Butler,L., Galanty,Y., Pangon,L., Kiuchi,T. *et al*. (2009) The SUMO modification pathway is involved in the BRCA1 response to genotoxic stress. *Nature*, **462**, 886–890.
31. Haince,J.F., McDonald,D., Rodrigue,A., Dery,U., Masson,J.Y., Hendzel,M.J. and Poirier,G.G. (2008) PARP1-dependent kinetics of recruitment of MRE11 and NBS1 proteins to multiple DNA damage sites. *J. Biol. Chem*., **283**, 1197–1208.
32. Ma,J.B., Yuan,Y.R., Meister,G., Pei,Y., Tuschl,T. and Patel,D.J. (2005) Structural basis for 5'-end-specific recognition of guide RNA by the A. fulgidus Piwi protein. *Nature*, **434**, 666–670.
33. Ziv,Y., Bar-Shira,A., Pecker,I., Russell,P., Jorgensen,T.J., Tsarfati,I. and Shiloh,Y. (1997) Recombinant ATM protein complements the cellular A-T phenotype. *Oncogene*, **15**, 159–167.
34. Lees-Miller,S.P., Godbout,R., Chan,D.W., Weinfeld,M., Day,R.S. 3rd, Barron,G.M. and Allalunis-Turner,J. (1995) Absence of p350 subunit of DNA-activated protein kinase from a radiosensitive human cell line. *Science*, **267**, 1183–1185.
35. Gagne,J.P., Hunter,J.M., Labrecque,B., Chabot,B. and Poirier,G.G. (2003) A proteomic approach to the identification of heterogeneous nuclear ribonucleoproteins as a new family of poly(ADP-ribose)-binding proteins. *Biochem. J*., **371**, 331–340.
36. Ismail,I.H., Martensson,S., Moshinsky,D., Rice,A., Tang,C., Howlett,A., McMahon,G. and Hammarsten,O. (2004) SU11752 inhibits the DNA-dependent protein kinase and DNA double-strand break repair resulting in ionizing radiation sensitization. *Oncogene*, **23**, 873–882.
37. Rodrigue,A., Lafrance,M., Gauthier,M.C., McDonald,D., Hendzel,M., West,S.C., Jasin,M. and Masson,J.Y. (2006) Interplay between human DNA repair proteins at a unique double-strand break *in vivo*. *EMBO J*., **25**, 222–231.
38. Chou,D.M., Adamson,B., Dephoure,N.E., Tan,X., Nottke,A.C., Hurov,K.E., Gygi,S.P., Colaiacovo,M.P. and Elledge,S.J. (2010) A chromatin localization screen reveals poly (ADP ribose)-regulated recruitment of the repressive polycomb and NuRD

complexes to sites of DNA damage. *Proc. Natl Acad. Sci. USA*, **107**, 18475–18480.
39. Pan,M.R., Peng,G., Hung,W.C. and Lin,S.Y. (2011) Monoubiquitination of H2AX protein regulates DNA damage response signaling. *J. Biol. Chem.*, **286**, 28599–28607.
40. Roscic,A., Moller,A., Calzado,M.A., Renner,F., Wimmer,V.C., Gresko,E., Ludi,K.S. and Schmitz,M.L. (2006) Phosphorylation-dependent control of Pc2 SUMO E3 ligase activity by its substrate protein HIPK2. *Mol. Cell*, **24**, 77–89.
41. Facchino,S., Abdouh,M., Chatoo,W. and Bernier,G. (2010) BMI1 confers radioresistance to normal and cancerous neural stem cells through recruitment of the DNA damage response machinery. *J. Neurosci.e*, **30**, 10096–10111.
42. Liu,J., Cao,L., Chen,J., Song,S., Lee,I.H., Quijano,C., Liu,H., Keyvanfar,K., Chen,H., Cao,L.Y. *et al.* (2009) Bmi1 regulates mitochondrial function and the DNA damage response pathway. *Nature*, **459**, 387–392.
43. Chagraoui,J., Hebert,J., Girard,S. and Sauvageau,G. (2011) An anticlastogenic function for the Polycomb Group gene Bmi1. *Proc. Natl Acad. Sci. USA*, **108**, 5284–5289.
44. Vincenz,C. and Kerppola,T.K. (2008) Different polycomb group CBX family proteins associate with distinct regions of chromatin using nonhomologous protein sequences. *Proc. Natl Acad. Sci. USA*, **105**, 16572–16577.
45. Krishnakumar,R. and Kraus,W.L. (2010) PARP-1 regulates chromatin structure and transcription through a KDM5B-dependent pathway. *Mol. Cell*, **39**, 736–749.
46. Haince,J.F., Kozlov,S., Dawson,V.L., Dawson,T.M., Hendzel,M.J., Lavin,M.F. and Poirier,G.G. (2007) Ataxia telangiectasia mutated (ATM) signaling network is modulated by a novel poly(ADP-ribose)-dependent pathway in the early response to DNA-damaging agents. *J. Biol. Chem.*, **282**, 16441–16453.
47. Koh,D.W., Lawler,A.M., Poitras,M.F., Sasaki,M., Wattler,S., Nehls,M.C., Stoger,T., Poirier,G.G., Dawson,V.L. and Dawson,T.M. (2004) Failure to degrade poly(ADP-ribose) causes increased sensitivity to cytotoxicity and early embryonic lethality. *Proc. Natl Acad. Sci. USA*, **101**, 17699–17704.
48. Gagne,J.P., Moreel,X., Gagne,P., Labelle,Y., Droit,A., Chevalier-Pare,M., Bourassa,S., McDonald,D., Hendzel,M.J., Prigent,C. *et al.* (2009) Proteomic investigation of phosphorylation sites in poly(ADP-ribose) polymerase-1 and poly(ADP-ribose) glycohydrolase. *J. Proteome Res.*, **8**, 1014–1029.
49. Bayer,P., Arndt,A., Metzger,S., Mahajan,R., Melchior,F., Jaenicke,R. and Becker,J. (1998) Structure determination of the small ubiquitin-related modifier SUMO-1. *J. Mol. Biol.*, **280**, 275–286.
50. Cao,R., Wang,L., Wang,H., Xia,L., Erdjument-Bromage,H., Tempst,P., Jones,R.S. and Zhang,Y. (2002) Role of histone H3 lysine 27 methylation in Polycomb-group silencing. *Science*, **298**, 1039–1043.
51. Fischle,W., Wang,Y., Jacobs,S.A., Kim,Y., Allis,C.D. and Khorasanizadeh,S. (2003) Molecular basis for the discrimination of repressive methyl-lysine marks in histone H3 by Polycomb and HP1 chromodomains. *Genes Dev.*, **17**, 1870–1881.
52. Min,J., Zhang,Y. and Xu,R.M. (2003) Structural basis for specific binding of Polycomb chromodomain to histone H3 methylated at Lys 27. *Genes Dev.*, **17**, 1823–1828.
53. van der Lugt,N.M., Domen,J., Linders,K., van Roon,M., Robanus-Maandag,E., te Riele,H., van der Valk,M., Deschamps,J., Sofroniew,M., van Lohuizen,M. *et al.* (1994) Posterior transformation, neurological abnormalities, and severe hematopoietic defects in mice with a targeted deletion of the BMI1 proto-oncogene. *Genes Dev.*, **8**, 757–769.
54. Johnson,E.S. (2004) Protein modification by SUMO. *Annual Rev. Biochem.*, **73**, 355–382.
55. Huber,A., Bai,P., de Murcia,J.M. and de Murcia,G. (2004) PARP-1, PARP-2 and ATM in the DNA damage response: functional synergy in mouse development. *DNA Repair*, **3**, 1103–1108.
56. Haince,J.F., McDonald,D., Rodrigue,A., Dery,U., Masson,J.Y., Hendzel,M.J. and Poirier,G.G. (2008) PARP1-dependent kinetics of recruitment of MRE11 and NBS1 proteins to multiple DNA damage sites. *J. Biol. Chem.*, **283**, 1197–1208.
57. Sustackova,G., Kozubek,S., Stixova,L., Legartova,S., Matula,P., Orlova,D. and Bartova,E. (2012) Acetylation-dependent nuclear arrangement and recruitment of BMI1 protein to UV-damaged chromatin. *J. Cell. Physiol.*, **227**, 1838–1850.